Published in IET Optoelectronics
Received on 5th March 2008
doi: 10.1049/iet-opt:20080009

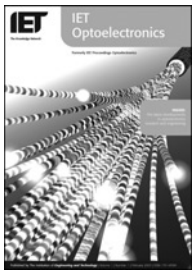

ISSN 1751-8768

Greatly reduced radiation loss in planar waveguides with two-dimensional conducting interfaces

P. Sarrafi N. Zareian K. Mehrany

Department of Electrical Engineering, Sharif University of Technology, PO Box, 11-365-863, Tehran, Iran
E-mail: mehrany@sharif.edu

Abstract: A new strategy for radiation loss reduction in curved slab waveguides is presented. The proposed strategy is based on the proper modification of the boundary conditions at the core-to-cladding interface, whereupon extremely thin conductive nanolayers with non-zero surface conductance are imposed. The obtained numerical results show a noticeable decrease in the overall loss level.

1 Introduction

Waveguide bends with small radii of curvature are needed to meet the increasing demands for small-scale device integration and exigencies of highly packed optical circuits. The desired smallest bending radius is nonetheless limited by the level of loss, which is mainly due to the radiation of the formerly guided modes and increases exponentially as the radius of curvature becomes smaller [1, 2]. Intensive research has been consequently carried out over the past few decades on various curved structures [3, 4], where much concentration is put into minimising the radiation loss as much as possible without sacrificing the bending curvature [5]. In principle, most of the proposed strategies so far resort to refractive index profile engineering, which is based on two basic yet similar principles [2]. First, the radiation loss can be reduced by tight confinement of electromagnetic fields within the core. This can be achieved most simply through an increase in the contrast between the core and the cladding refractive index [1], for example, by decreasing the outer refractive index [6], or by applying micro-prisms of raised index along the waveguide path [7–10]. Secondly, the leakage attenuation can be decreased by driving the radiation caustic farther off the core. This latter strategy can be implemented by using isolation trenches [11–14], or more subtle arrangements of multiple claddings [2, 15–17], whereupon the evanescent modal field amplitude at the receded radiation caustic and consequently, the radiation loss are both reduced [18].

In this paper, a different approach is adopted, where the boundary conditions at the outer or at the inner boundaries of the core region are duly modified by imposing conducting interfaces, that is, extremely thin conductive nanolayers with surface conductance σ_s. These conducting interfaces can be realised by using two-dimensional free charge layers [19] or possibly thin sheets of graphene [20]. In contrast to the conventional refractive index profile engineering, here, we try to change the bending loss by varying the boundary conditions, where the tangential components of the electric field at the conducting interface produce a proportional surface current density imposing a discontinuity upon the otherwise continuous tangential magnetic field [19, 21–24]. This controlled discontinuity of the tangential magnetic field can then considerably reduce the bend loss by using either of the following mechanisms. First, conducting interface can support the surface electromagnetic waves [19, 22, 24], confine the electromagnetic energy and reduce the radiation loss. Secondly, the conducting interface can increase the reflection coefficient of the outer boundary and take the part of a reflector placed at the outer edge of the core. This latter mechanism does not change the radius of the radiation caustic; yet, effectively decreases the diffractive tunnelling in frustrated total internal reflection.

Organisation of this paper is as follows: the mathematical formulation for the TE wave propagation in a bent slab structure is discussed in Section 2. The proposed approach

is, however, general and can be similarly followed for the analysis of the TM wave propagation in any planar structure with discrete refractive index variations. In Section 3, bent loss reduction in a typical planar structure with conducting interface is numerically studied. Electric field profiles of different leaky modes are also presented and the underlying physics of bent loss reduction is briefly revealed. Further considerations are given in Section 4. Finally, conclusions are made in Section 5.

2 Formulation

A number of methods have been reported for the analysis of curved waveguides [25–35]. Here, we follow a rigorous modal analysis, where electromagnetic fields are given in terms of Bessel and Hankel functions, that is, the exact solution of Helmholtz equation with piecewise constant refractive indices in cylindrical coordinates (r, ϕ, z). In the following, we consider TE polarised waves propagating in a bent planar waveguide, which is geometrically invariant with respect to ϕ. The transverse electric field E_z then assumes the following form [36]

$$E_z = S(r)\exp(-\mathrm{j}\beta r_0\phi) \tag{1}$$

where β stands for the complex propagation constant of the wave and $S(r)$ is governed by the following equation [27]

$$\frac{1}{r}\frac{\partial}{\partial r}\left(r\frac{\partial S}{\partial r}\right) - \frac{\beta^2 r_0^2}{r^2}S + k_0^2 n^2(r)S = 0 \tag{2}$$

Here, k_0 represents the wavenumber in vacuum and r_0 denotes the central curvature radius shown in Fig. 1. In this structure, where the refractive index profile $n(r)$ is constant within radial intervals $r < r_1$, $r_1 < r < r_2$ and $r_2 < r$, the general solution of (2) can be easily written in terms of Bessel and Hankel functions [36]

$$S = \begin{cases} CJ_\nu[k_0 n_0 r], & r < r_1 \\ AH_\nu^{(1)}[k_0 n_1 r] + BH_\nu^{(2)}[k_0 n_1 r], & r_1 \le r \le r_2 \\ DH_\nu^{(2)}[k_0 n_0 r], & r_2 < r \end{cases} \tag{3}$$

Although the appropriate conditions at singular end points, that is, at $r \to 0$ and $r \to \infty$, are already put into the preceding functional form, the governing boundary conditions for tangential electromagnetic fields at the inner and outer boundaries, that is, at $r = r_1$ and $r = r_2$, remain to be applied. These conditions read as [13, 24]

$$\begin{cases} E_z(r_i^+) = E_z(r_i^-), \\ H_\phi(r_i^+) - H_\phi(r_i^-) = \sigma_{s,i}E_z, \end{cases} \quad i = 1, 2 \tag{4}$$

where $\sigma_{s,i}$ represents the conductance of two-dimensional charge carriers imposed at the interface $r = r_i$. It can be described by using the Drude-like expression for conventional 2D electron/hole gas systems, for example, in GaAs/GaAlAs quantum-well structures, or the Dirac spectrum for massless electrons in graphene sheets [22].

To facilitate future calculations, surface conductance σ_i is normalised to intrinsic wave impedance, whereupon α_i, that is, normalised surface conductivity, is introduced

$$\sigma_{s,i} = -\mathrm{j}\left(\frac{\varepsilon_0}{\mu_0}\right)^{1/2}\alpha_i \tag{5}$$

Although essentially a complex number, σ_i is almost imaginary at terahertz frequencies at which the scattering rate of 2D charge carriers can be neglected. This also holds true in graphene sheets, where the damping effects are shown to be negligible even at the room temperature [22]. Therefore α_i is practically an almost a real number.

Now, applying the appropriate boundary conditions (4) to the proposed ansatz for $S(r)$, and after some algebraic manipulations, the non-trivial solution can be found only under a certain condition, which is governed by the dispersion equation.

Inspection of this equation clearly reveals that non-zero surface conductance, that is, $\alpha_i \neq 0$, can substantially change the overall electromagnetic behaviour and consequently, the modal behaviour. This can be physically understood in terms of the created surface current density, which obviously imposes a certain discontinuity upon the formerly continuous tangential magnetic field. Such possible alterations are further discussed through various numerical examples in the next two sections

$$M = \begin{bmatrix} H_\nu^1[k_0 n_1 r_1] & H_\nu^2[k_0 n_1 r_1] & -J_\nu[k_0 n_0 r_1] & 0 \\ n_1 H_\nu^{1'}[k_0 n_1 r_1] & n_1 H_\nu^{2'}[k_0 n_1 r_1] & -n_0 J_\nu'[k_0 n_0 r_1] & 0 \\ & & -\alpha_1 J_\nu[k_0 n_0 r_1] & \\ H_\nu^1[k_0 n_1 r_2] & H_\nu^2[k_0 n_1 r_2] & 0 & -H_\nu^2[k_0 n_0 r_2] \\ n_1 H_\nu^{1'}[k_0 n_1 r_2] & n_1 H_\nu^{1'}[k_0 n_1 r_2] & 0 & -n_0 H_\nu^{2'}[k_0 n_0 r_2] + \alpha_2 H_\nu^2[k_0 n_0 r_2] \end{bmatrix} \tag{6}$$

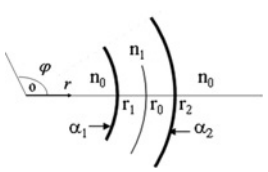

Figure 1 *Bent waveguide with central radius r_0*

3 Bend loss reduction

In this section, different bend loss reduction mechanisms based on non-zero surface conductance are investigated by numerically studying a typical bent planar waveguide with the following parameters: $r_2 - r_1 = 4\lambda$, $r_0 = 2000\lambda$, $n_1 = 1.503$ and $n_0 = 1.5$. Although a special case, this example clearly demonstrates how the bend loss can be largely reduced by using the non-zero surface conductance. It also provides the basic understanding of the main physical principles behind the observed benefits of using the proposed strategy. Clearly, either or both of the interfaces can be conductive, yet, the outer interface at $r = r_2$, whereof the electromagnetic energy radiates away, is here chosen to have a non-zero surface conductance, that is, $\alpha_2 \neq 0$. Numerical study of the most general case is therefore deferred to next section, where more complicated combinations are considered.

3.1 Radiation loss reduction in the principal mode

Here, the propagation constant of the first-order leaky mode in the aforementioned structure is more closely examined. In Fig. 2, the attenuation level of total loss, that is, the imaginary part of the propagation constant β, is plotted against the real and imaginary parts of the normalised surface conductivity α_2. The imaginary part of the normalised surface conductivity is always positive, as it represents the inevitable loss. The real part of the normalised surface conductivity, in contrast, could be either positive or negative. If it is positive, then conventional Drude-like electrons, for instance, in GaAs/AlGaAs quantum well structures, are involved [22]. If it is negative, the overall surface conductivity mainly consists of the inter-band contribution, as it could be the case in graphene sheets [22].

Inspection of this figure, however, reveals several interesting features. These features can be easily understood in terms of the electromagnetic role that non-zero surface conductivity plays.

In case the imaginary part of surface conductivity is positive, that is, the real part of α_2 is negative, electromagnetic energy has a propensity to be localised [19, 21, 22] and exhaustive radiation loss could therefore be prevented. This can be easily seen by the comparison of Figs. 3 and 4, which show the electric field profiles of the first-order leaky mode, respectively, with $\alpha_2 = 0$ and -0.2. Although the above-mentioned electromagnetic confinement can considerably abate the radiation loss level, it is inherently sensitive to the imaginary part of α_2, that is, the ohmic loss that the confined wave is now doomed to encounter while propagating along the interface. This point is clearly demonstrated in the zoomed-in inlay of Fig. 2, where the attenuation level is shown to sharply rise as the imaginary part of α_2, that is, the real part of surface conductivity representing the ohmic loss, increases.

In case the imaginary part of surface conductivity is negative, that is, the real part of α_2 is positive, electromagnetic energy cannot be localised to cause any drastic change of radiation loss. Nevertheless, the presence of positive α_2 increases the electromagnetic reflection coefficient of the boundary whereupon a conducting sheet is introduced [37]. Therefore the electromagnetic energy of the wave will be pushed back to the core, whence the diffractive tunnelling in frustrated total internal reflection will be further decreased.

This is clearly demonstrated in Figs. 5*a* and 5*b*, which show the electric field profile with $\alpha_2 = 0.2$ and 1, respectively. Concentration of electromagnetic energy in the core, as it is shown in Fig. 5, explains the relatively low sensitivity of the overall radiation loss to the imaginary part of α_2, that is, the ohmic loss.

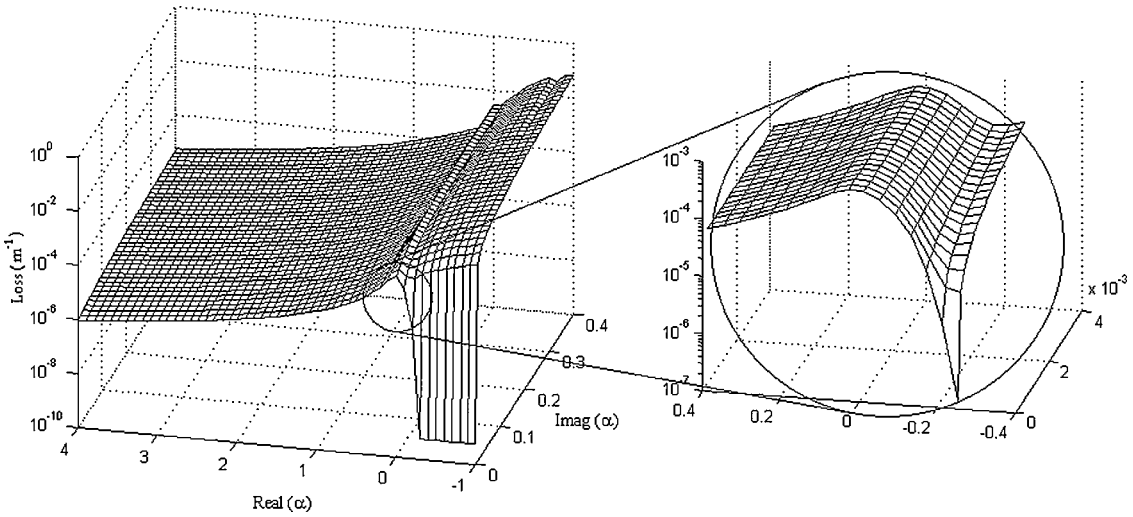

Figure 2 *Attenuation level of loss for the first-order leaky mode against the real and imaginary parts of* α

doi: 10.1049/iet-opt:20080009

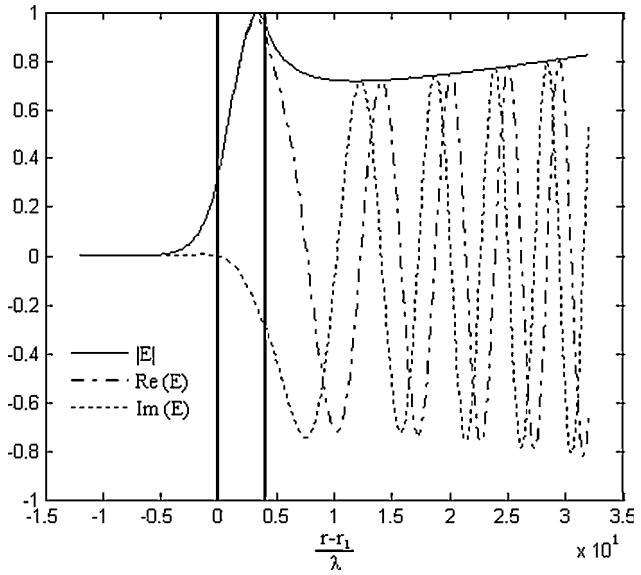

Figure 3 *Electrical wavefunction of first mode against $r-r_1$ with $\alpha_1 = \alpha_2 = 0$, $\beta_1/k_0 = 1.5021 - 4.725 \times 10^{-4}\ i$*
Inner and outer boundaries are shown by using solid lines

Two different mechanisms are therefore perceptible. In the first mechanism, electromagnetic energy is more strongly bound at the outer interface than it formerly was. Although the radiation loss is drastically decreased in this fashion, the ohmic loss, which is inevitably incurred, is likely to become the dominant loss factor. In the second mechanism, however, the electromagnetic energy is pushed back to the core, where the ohmic loss of conducting layers cannot cause much trouble.

These mechanisms are controlled by the algebraic sign of the real part of the normalised surface conductivity, which happens to be a crucial factor in determining how the overall loss level will change.

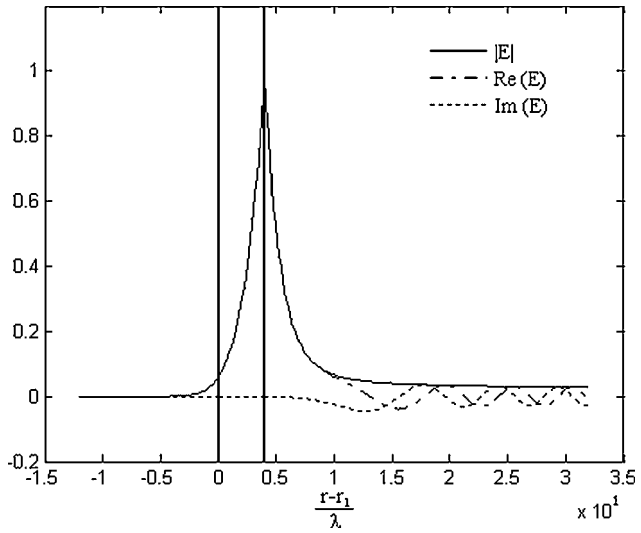

Figure 4 *Electrical wavefunction of first mode against $r-r_1$ with $\alpha_1 = 0$, $\alpha_2 = -0.2$: $\beta_1/k_0 = 1.5064 - 5.386 \times 10^{-6}\ i$*

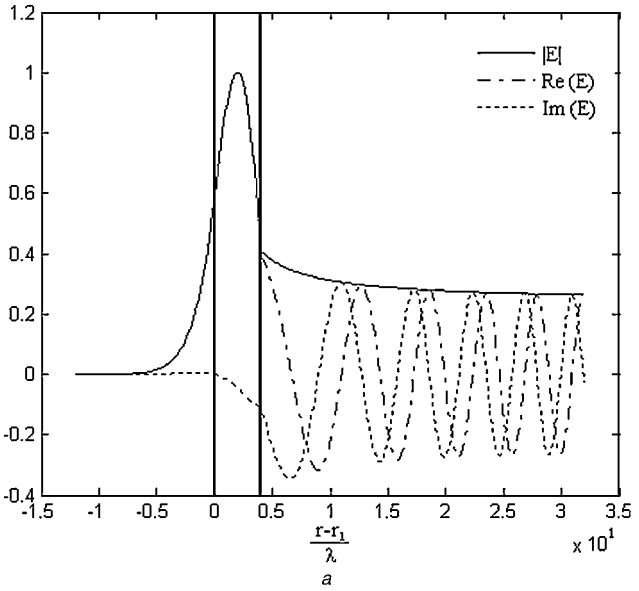

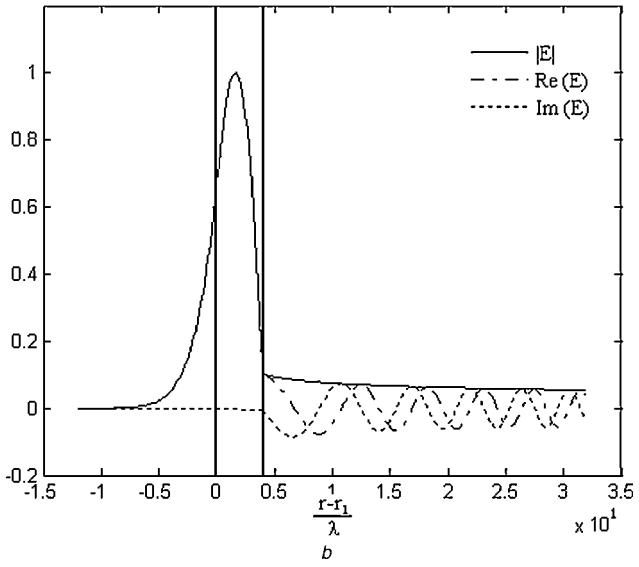

Figure 5 *Electrical wavefunction of first mode against $r-r_1$ with*
a $\alpha_1 = 0$, $\alpha_2 = 0.2$, $\beta_1/k_0 = 1.5006 - 1.714 \times 10^{-4}\ i$
b $\alpha_1 = 0$, $\alpha_2 = 1$, $\beta_1/k_0 = 1.5001 - 1.312 \times 10^{-5}\ i$

3.2 Radiation loss reduction in the second mode

This section is devoted to the propagation constant of the second-order leaky mode in the aforementioned structure. In Fig. 6, the attenuation level of loss is similarly plotted against the real and imaginary parts of the normalised surface conductivity α_2. Although the preceding mechanisms are still working, the observed radiation loss reduction conspicuously differs when the second-order mode is considered. This difference, which is strong enough to kill one mode and keep the other, can be understood by noting that the electromagnetic profile of the second-order mode has two antinodes and is consequently harder to confine. As a result, the overall loss

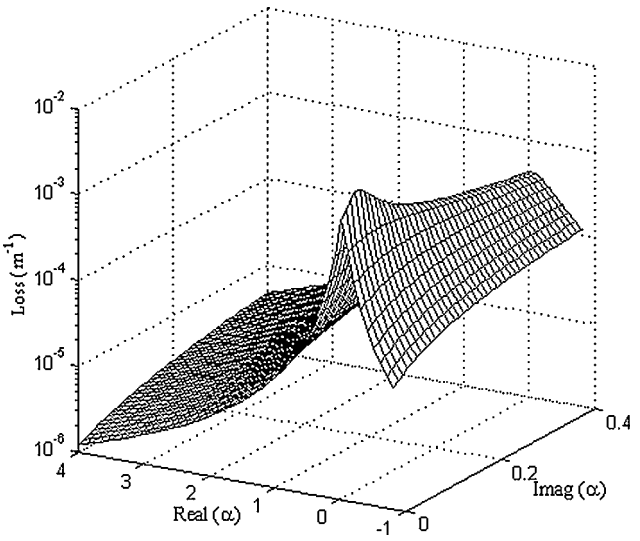

Figure 6 *Loss against real and imaginary parts of α for the second leaky mode*

level is not much sensitive to the ohmic loss incurred by introducing surface conductivity. This is clearly shown in Fig. 6, where the increase of the imaginary part of α_2 does not cause any sharp rise in the observed attenuation level even if the real part of α_2 is negative.

In Fig. 7, the transverse electric field profile of the second-order mode is plotted with $\alpha_2 = 0$. This figure clearly demonstrates why the second-order mode is lossier than the principal mode.

4 Further considerations

In this section, we consider the most general case where both the boundaries at $r = r_1$ and $r = r_2$ are assumed conducting, that is, $\alpha_1 \neq 0$ and $\alpha_2 \neq 0$.

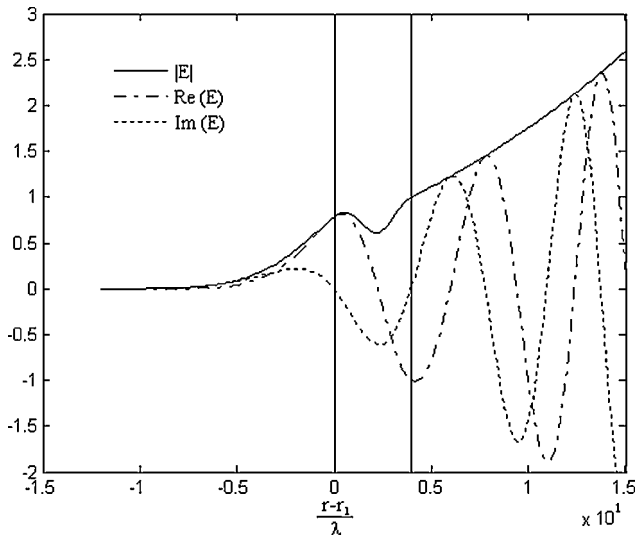

Figure 7 *Electrical wavefunction of second mode against $r - r_1$ with $\alpha_1 = \alpha_2 = 0$, $\beta_2/k_0 = 1.4972 - 1.814 \times 10^{-3}i$*

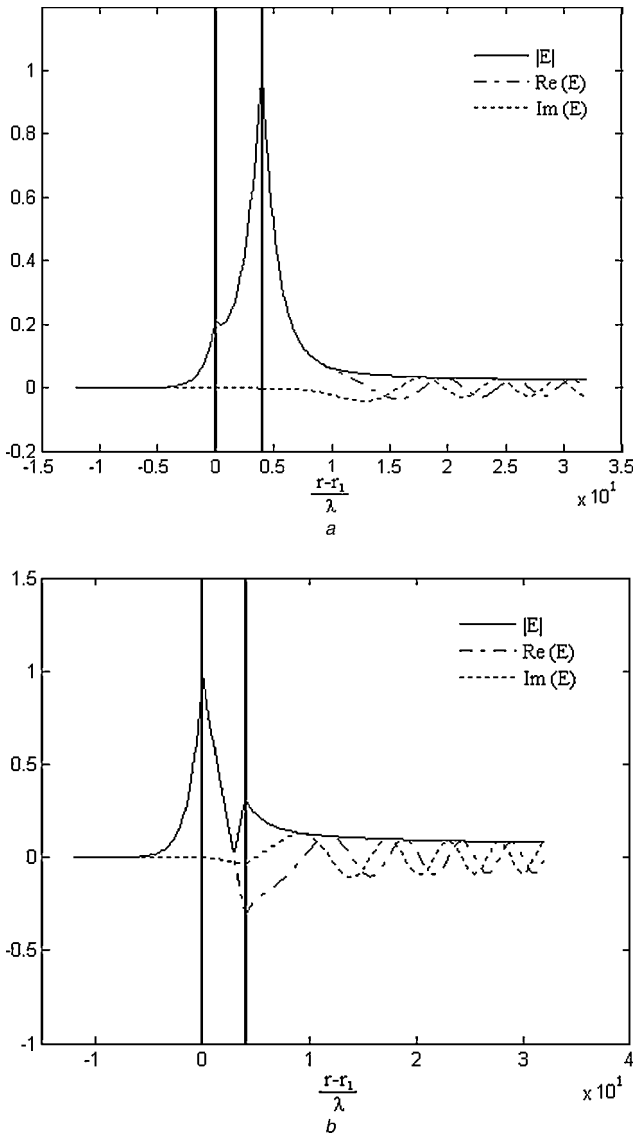

Figure 8 *Electric field profile*

a Electric field profile of the first-order mode propagating in the last structure with $\alpha_1 = -0.2$ and $\alpha_2 = -0.2$ is plotted: $\beta_1/k_0 = 1.5064 - 4.451 \times 10^{-6}i$

b Electric field profile of the second-order modes propagating in the last structure with $\alpha_1 = -0.2$ and $\alpha_2 = -0.2$ is plotted: $\beta_2/k_0 = 1.5032 - 4.436 \times 10^{-5}i$

In case the inner boundary is conducting and the real part of the normalised surface conductivity is positive, then the electromagnetic energy will be expelled forward whence it more easily radiates away. This can be explained by the increased reflection from the core to inner cladding interface. Therefore the real part of the normalised surface conductivity at $r = r_1$ should be always negative or else the overall loss level increases.

As the presence of negative α_1 results in further confinement of the electromagnetic energy, combination of two conducting interfaces with negative normalised surface conductivities at $r = r_1$ and $r = r_2$ is expected to decrease the overall loss level. This combination, however, is much

doi: 10.1049/iet-opt:20080009

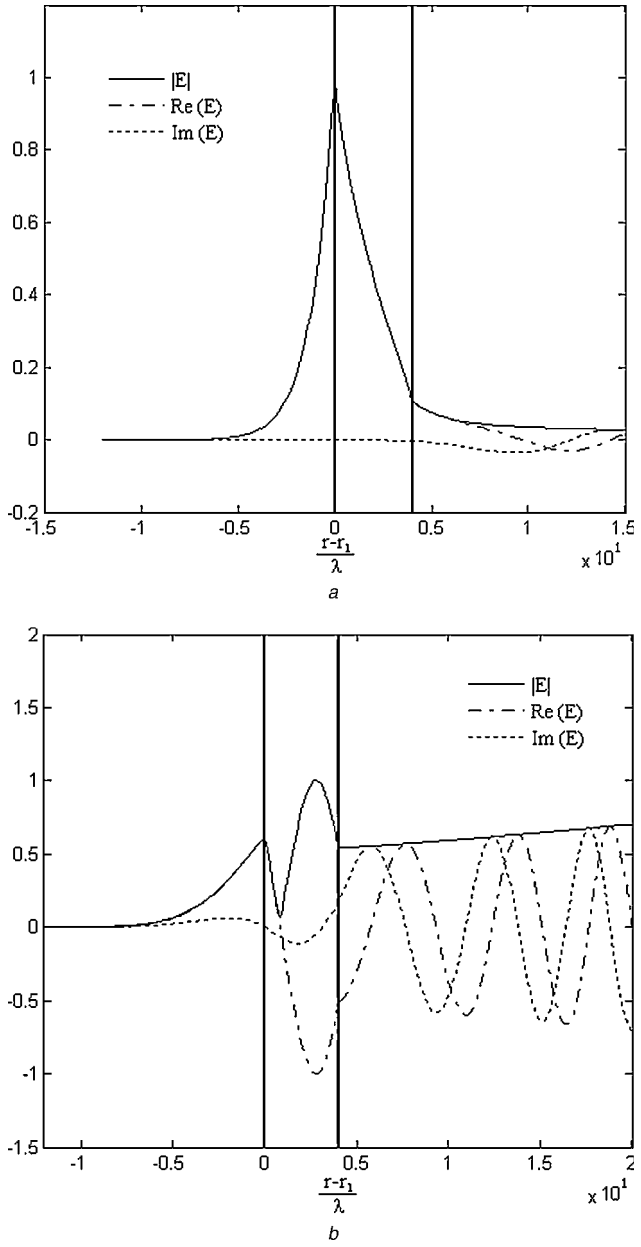

Figure 9 *Electric field profile*

a Electric field profile of the first-order mode propagating in the last structure with $\alpha_1 = -0.2$ and $\alpha_2 = +0.2$ is plotted: $\beta_1/k_0 = 1.5037 - 3.0447 \times 10^{-6}i$

b Electric field profile of the second-order mode propagating in the last structure with $\alpha_1 = -0.2$ and $\alpha_2 = +0.2$ is plotted: $\beta_1/k_0 = 1.4977 - 6.6495 \times 10^{-4}i$

more effective for the second-order leaky mode, where the presence of two antinodes makes energy confinement more difficult to achieve. This is clearly shown in Figs. 8*a* and 8*b*, where the electric field profile of the first- and second-order modes propagating in the same structure with $\alpha_1 = -0.2$ and $\alpha_2 = -0.2$ are plotted.

Similarly, the combination of negative α_1 and positive α_2 brings forth a slight improvement over the case, where $\alpha_1 = 0$ and the real part of the normalised surface conductivity at $r = r_2$ is positive. This is demonstrated in Figs. 9*a* and 9*b*, where the electric field profile of the first- and second-order modes propagating in the same structure with $\alpha_1 = -0.2$ and $\alpha_2 = 0.2$ are plotted.

5 Conclusion

In this paper, extremely thin conductive nanolayers with non-zero surface conductance σ_s are employed to alter the electromagnetic boundary conditions at the core-to-cladding interface. In this fashion, the radiation loss of the curved structure can be reduced because of two different reasons. First, the electromagnetic energy could be further confined to the core. Secondly, the reflection coefficient of the outer interface could be increased to frustrate the electromagnetic tunnelling. Different numerical examples are given, unfavourable effects of the ohmic loss are taken into account and the presented results are intuitively interpreted.

6 References

[1] LADOUCEUR E., LOVE J.D.: 'Silica based buried channel waveguides and devices' (Chapman & Hall, London, 1996)

[2] TOMLJENOVIC-HANIC S., LOVE J.D., ANKIEWICZ A.: 'Effect of additional layers on bend loss in buried channel waveguides', *IEE Proc., Optoelectron.*, 2003, **150**, (3), pp. 259–265

[3] LEWIN L., CHANG D.C., KUESTER E.F.: 'Electromagnetic waves and curved structures, 'IEE Electromagnetic Waves Series' (Peter Peregrinus, Ltd., Stevenage, Herts, England, 1997), vol. 2, p. 205

[4] SPORLEDER F., UNGER H.G.: 'Waveguides tapers transitions and couplers' (IEE-Press, Peter Peregrinus Ltd., Steveage London, 1979)

[5] NEUMANN E.G., RICHTER W.: 'Sharp bends with low losses in dielectric optical waveguides', *Appl. Opt.*, 1983, **22**, pp. 1016–1022

[6] MAJD M., SCHUPPERT B., PETERMANN K.: '90° S-bends in Ti:$LiNbO_3$ waveguides with low losses', *IEEE Photonics Technol. Lett.*, 1993, **5**, pp. 806–808

[7] HIRAYAMA K., KOSHIBA M.: 'A new low-loss structure of abrupt bends in dielectric waveguides', *J. Lightwave Technol.*, 1992, **10**, pp. 563–569

[8] KOROTKY S.K., MARCATILI E.A.J., VESELKA J.J., BOSWORTH R.H.: 'Greatly reduced losses for small-radius bands in Ti:$LiNbO_3$ waveguides', *Appl. Phys. Lett.*, 1986, **48**, (2), pp. 92–94

[9] LIN H.B., SU J.Y., WEI P.K., WANG W.S.: 'Design and application of very low-loss abrupt bends in optical waveguides', *IEEE J. Quantum Electron.*, 1994, **30**, pp. 2827–2835

[10] LU R.C., LIAO Y.P., LIN H.B., WANG W.S.: 'Design and fabrication of wide-angle abrupt bends on lithium niobate', *IEEE J. Sel. Top. Quantum Electron.*, 1996, **2**, pp. 215–220

[11] YAMAUCHI J., IKEGAYA M., NAKANO H.: 'Bend loss of step-index slab waveguides with a trench section', *Microw. Opt. Technol. Lett.*, 1992, **5**, (6), pp. 251–254

[12] SEO C., CHEN J.C.: 'Low transition losses in bent rib waveguides', *J. Lightwave Technol.*, 1996, **14**, (10), pp. 2255–2259

[13] RAJARAJAN M., OBAYYA S.S.A., RAHMAN B.M.A., GRATTAN K.T.V., EL-MIKATI H.A.: 'Design of compact optical bends with a trench by use of finite-element and beam-propagation methods', *Appl. Opt.*, 2000, **39**, pp. 4946–4953

[14] POPOVIC M., WADA K., AKIYAMA S., HAUS H.A., MICHEL J.: 'Air trenches for sharp silica waveguides bends', *J. Lightwave Technol.*, 2002, **20**, (9), pp. 1762–1772

[15] TOMLJENOVIC-HANIC S., LOVE J.D., ANKIEWICZ A.: 'Low-loss single mode waveguide and fiber bends', *Electron. Lett.*, 2002, **38**, (5), pp. 220–222

[16] KAWAKAMI S., MIYAGI M., NISHIDA S.: 'Bending losses of dielectric slab optical waveguide with double or multiple claddings: theory', *Appl. Opt.*, 1975, **14**, (11), pp. 2588–2597

[17] TOMLJENOVIC-HANIC S., BULLA D.A.P., ANKIEWICZ A., LOVE J.D., BAILEY R.: 'Multiple-cladding fibers with reduced bend loss', *J. Opt. Soc. Am. A*, 2007, **24**, (4), pp. 1172–1176

[18] HEALY N., HUSSEY C.D.: 'Minimizing bend loss by removing material inside the caustic in bent single-mode fibers', *Appl. Opt.*, 2006, **45**, (18), pp. 4219–4222

[19] MEHRANY K., KHORASANI S., RASHIDIAN B.: 'Novel optical devices based on surface wave excitation at conducting interfaces', *Semicond. Sci. Technol.*, 2003, **18**, pp. 582–588

[20] BERGER C., SONG Z., LI T., *ET AL.*: 'Ultrathin epitaxial graphite: 2D electron gas properties and a route toward graphene-based nanoelectronics', *J. Phys. Chem. B*, 2004, **108**, (52), pp. 19912–19916

[21] MEHRANY K., RASHIDIAN B.: 'Novel optical slow wave structure and surface electromagnetic wave coupler with conducting interfaces', *Semicond. Sci. Technol.*, **19**, pp. 890–896

[22] MIKHAILOV S.A., ZIEGLER K.: 'New electromagnetic mode in graphene', *Phys. Rev. Lett.*, 2007, **99**, pp. 0168031–0168034

[23] SLEPYAN G.Y., MAKSIMENKO S.A., LAKHTAKIA A., YEVTUSHENKO O., GUSAKOV A.V.: 'Electrodynamics of carbon nanotubes: dynamic conductivity. Impedance boundary conditions, and surface wave propagation', *Phys. Rev. B*, 1999, **60**, pp. 17136–17149

[24] HANSON G.W.: 'Dyadic Green's functions and guided surface waves on graphene'. URSI North American Radio Science Meeting, Ottawa, Canada, July 2007

[25] MARCUSE D.: 'Bending loss of the asymmetric slab waveguides', *Bell Syst. Technol. J.*, 1971, **50**, p. 2551

[26] MARCATILI E.A.J.: 'Bends in optical dielectric guides', *Bell Syst. Tech. J.*, 1969, **48**, p. 2103

[27] JEDIDI R., PIERRE R.: 'Efficient analytical and numerical methods for the computation of bent loss in planar waveguides', *J. Lightwave Technol.*, 2005, **23**, pp. 2278–2284

[28] KIM W., KIM C.: 'Radiation losses of bent planar waveguides', *Fiber Integr. Opt.*, 2002, **21**, pp. 219–232

[29] HEIBLUM M., HARRIS J.H.: 'Analysis of curved optical waveguides by conformal transformation', *IEEE J. Quantum Electron.*, 1975, **QE-11**, pp. 75–85

[30] MARCUSE D.: 'Curvature loss formula for optical fibers', *J. Opt. Soc. Am.*, 1976, **66**, pp. 216–220

[31] MELLONI A., CARNIEL F., COSTA R., MARTINELLI M.: 'Determination of bend mode characteristics in dielectric waveguides', *J. Lightwave Technol.*, 2001, **19**, p. 571

[32] THYAGARAJAN K., SHENOY M.R., GHATAK A.K.: 'Accurate numerical method for the calculation of bending loss in optical waveguides using a matrix approach', *Opt. Lett.*, 1987, **12**, pp. 296–298

[33] BERGLUND W., GOPINATH A.: 'WKB analysis of bend losses in optical waveguides', *J. Lightwave Technol.*, 2000, **18**, pp. 1161–1166

[34] KIM C., KIM Y., KIM W.: 'Leaky modes of circular slab waveguides: modified airy functions', *IEEE J. Sel. Top. Quantum Electron.*, 2002, **8**, pp. 1239–1245

[35] SARRAFI P., ZAREIAN N., MEHRANY K.: 'Analytical extraction of leaky modes in circular slab waveguides with arbitrary refractive index profile', *Appl. Opt.*, 2007, **46**, (36), pp. 8656–8667

[36] HIREMATH K.R., HAMMER M., STOFFER R., PRKNA L., CTYROKY J.: 'Analytic approach to dielectric optical bent slab waveguides', *Opt. Quantum Electron.*, 2005, **37**, pp. 37–61

[37] MEHRANY K., RASHIDIAN B.: 'Asymptotic behavior of a subwavelength nanoconducting layer', *J. Opt. A, Pure Appl. Opt.*, 2006, **8**, pp. 639–646

doi: 10.1049/iet-opt:20080009